Realization of Even Transmission Zeros for Filter Without Cross-Couplings

Tianliang Zhang, *Member, IEEE*, Zhihe Long, Liguo Zhou, Man Qiao, Fangyan Hou, and Mingen Tian

***Abstract*— A new method is proposed to produce even finite transmission zeros without any cross-coupling between the resonators of filter, by loading the second-order extracted-pole unit (EPU) composed of two mutual coupled resonators at the input or output port of the filter. An arbitrary distribution of finite transmission zeros on the imaginary axis can be achieved by adjusting the resonant frequencies of resonators in the EPUs and the coupling strength between them. The finite transmission zeros can be symmetrically or asymmetrically distributed about the center frequency of the filter, even all on the same side outside the passband of the filter. And the topological structures of these filters are given in this paper. Besides, Cauchy method is adopted to analyze the proposed EPU configuration filter as well. This paper not only discusses how to implement a pair and two pairs of finite transmission zeros, and how to control the distribution of finite transmission zeros, but also gives multiple sets of computer-aided synthesized normalized coupling matrices. Based on this, an eighth-order quasi-elliptic function high-temperature superconducting filter with two pairs of finite transmission zeros was designed on a double-sided YBCO/$LaAlO_3$/YBCO films to verify the feasibility of this new structure.**

***Index Terms*— Filter, high-temperature superconducting (HTS), none cross-coupling, quasi-elliptic function, transmission zero.**

I. Introduction

STRONG anti-interference ability has become one of the very important properties of contemporary communication systems. In a wireless communication system, signal interference will cause a reduction in the coverage of communication base station, a sharp decline in communication capacity, a substantial degradation in signal quality, and even paralyze the communication system. In order to suppress the interference of the adjacent channel signals and improve the utilization of frequency resources as effectively as possible, the modern communication receiver front-end usually use the high selectivity filters. In order to use the low-order filters to realize a steep out-of-band rejection, introducing finite transmission zeros is a common approach [1]–[7]. Currently, loading cross-coupling between nonadjacent resonators is one of the widely used methods to produce transmission zeros. A lot of double-row filter structures and some complex filter structures for adding cross-coupling are put forward in both planar and cavity filter designs after many scholars' researches, such as canonical structure, cascaded triplet (CT) structure, and cascaded quadruplet structure [8]–[22]. But these structures may cause the filters to possess a big size or an irregular shape, which makes them not conducive to the integration in the system. Subsequently, regarding the planar circuits, some researchers are gradually inclined to use narrow cross-coupling lines to introduce cross-couplings between the nonadjacent resonators for a compact size [23]–[29]. But adopting this method faces several problems sometimes. For example, some special structure resonators and circuit layouts need to be applied to avoid introducing another unnecessary additional coupling as well, which will make the filter design inconvenient. And very thin cross-coupling line is required to realize a filter with a large fractional bandwidth even in the design of narrowband filters, so processing errors often make the filter with cross-coupling line have low processing success rate, and the processing repeatability is also not satisfactory. In [30]–[32], another approach to produce transmission zeros without adopting cross-coupling between nonadjacent resonators is presented, and it is found that when the coupling coefficients depend on frequency, the coupled-resonator filters can produce transmission zeros at finite frequencies.

In this paper, a design method of producing even finite transmission zeros without any cross-coupling is presented as well, and some new in-line topologies to expand the design flexibility for high-performance quasi-elliptic function filters is provided. It is mainly achieved by loading the extracted-pole unit (EPU) composed of two mutually coupled resonators at the input or output of the filter to generate a pair or even more pairs of finite transmission zeros. And adjusting the resonant frequencies of the resonators in the EPUs and the coupling strengths between the resonators in EPUs can achieve arbitrary distribution of the finite transmission zeros. Also, because there is no cross-coupling between nonadjacent resonators, some complicated cross-coupling structures are naturally not considered. The resonators can be any shape, and the entire design process of the filter will be just like the traditional simple Chebyshev filter design process.

II. Topology of the New Quasi-Elliptic Function Filter

The conventional Chebyshev filter topology is shown in Fig. 1(a), including an input port S, an output port L,

Manuscript received February 8, 2018; revised April 27, 2018 and July 25, 2018; accepted August 18, 2018. Date of publication October 4, 2018; date of current version December 11, 2018. This work was supported by the Natural Science Foundation of China under Project 61471094. *(Corresponding author: Tianliang Zhang.)*

T. Zhang, L. Zhou, F. Hou, and M. Tian are with the School of Aeronautics and Astronautics, University of Electronic Science and Technology of China, Chengdu 611731, China (e-mail: ztl@uestc.edu.cn).

Z. Long and M. Qiao are with the School of Communication and Information Engineering, University of Electronic Science and Technology of China, Chengdu 611731, China.

Color versions of one or more of the figures in this paper are available online at http://ieeexplore.ieee.org.

Digital Object Identifier 10.1109/TMTT.2018.2871140

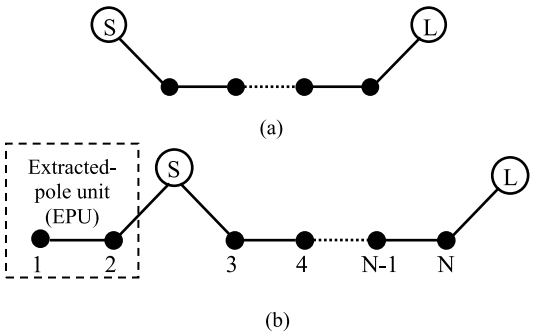

Fig. 1. Structure of quasi-elliptic function filter. (a) Traditional Chebyshev filter topology. (b) Quasi-elliptic function filter topology loaded proposed EPU.

TABLE I

NORMALIZED COUPLING MATRIX OF SIXTH-ORDER QUASI-ELLIPTIC FUNCTION FILTER WITH ONE PAIR OF FINITE TRANSMISSION ZEROS

	S	1	2	3	4	5	6	L
S	0	0	1.5871	0.8594	0	0	0	0
1	0	0	1.8866	0	0	0	0	0
2	1.5871	1.8866	0	0	0	0	0	0
3	0.8594	0	0	0	0.6567	0	0	0
4	0	0	0	0.6567	0	0.6504	0	0
5	0	0	0	0	0.6504	0	0.9280	0
6	0	0	0	0	0	0.9280	0	1.0885
L	0	0	0	0	0	0	1.0885	0

and several resonators arranged in order. Currently, in order to introduce finite transmission zeros outside the passband of the filter, in addition to adding cross-coupling between nonadjacent resonators, there is also an approach of loading an extracted-pole resonator at the input or output of the conventional Chebyshev filter, and the extracted-pole resonator concludes a phase shifter and a dedicated resonator [33]–[38]. And this method is sometimes called the extracted-pole technique, but only one finite transmission zero can be produced every time by loading this kind of extracted-pole resonator. In this paper, a new kind of EPU consisting of two resonators (Resonator 1 and Resonator 2) is proposed and by loading it at the input or output as shown in Fig. 1(b), one (two) pair(s) of finite transmission zero(s) can be generated, so it can realize quasi-elliptic function filter design without any cross-coupling. And the mechanism of introducing finite transmission zeros of the proposed EPU configuration is the same as that of the conventional extracted-pole technique. In Fig. 1(b), the frequencies of Resonator 1 and Resonator 2 are the same with or close to each other, and there exists coupling between Resonator 1 and Resonator 2.

According to the topology structure in Fig. 1(b), a set of sixth-order filter ($N = 6$) normalized coupling matrix are synthesized by optimization in Table I. In general, the synthesis of the coupling matrix can be derived from the transfer and reflection polynomials of the filter [36]. However, the procedure is relatively complex. In order to realize the fast design of the new EPU structure filter, the computer optimization technique is actually adopted to synthesize the coupling matrix. And in the process of synthesis, the design of the EPU structure filter's main signal path is consistent with the conventional

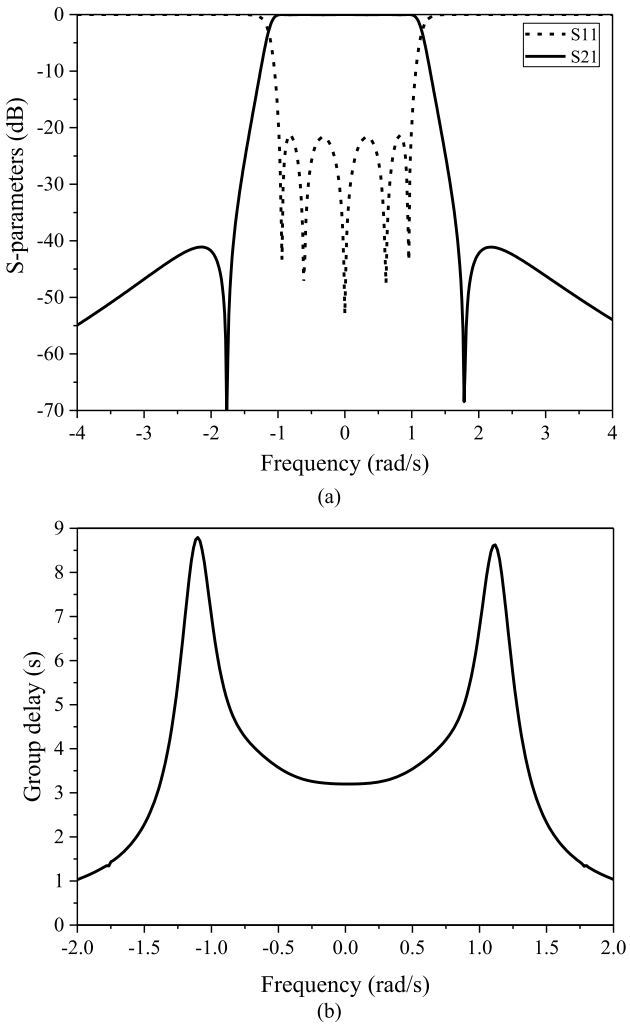

Fig. 2. Analysis of sixth-order quasi-elliptic function with one pair of finite transmission zero coupling matrix. (a) S-parameters. (b) Group delay.

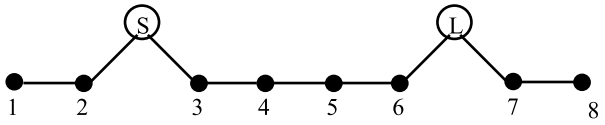

Fig. 3. Topology structure of eighth-order quasi-elliptic function filter with two pairs of finite transmission zeros.

Chebyshev filter design. Only the selection of the initial values of EPU needs to be paid attention to the following three points: first, the frequencies of the two resonators in the proposed EPU are set to be the same as the central frequency of the filter; second, the coupling strength between these two resonators is chosen to be an appropriate value according to the positions of the transmission zeros required by the prescribed filter specifications; and third, the coupling between the input (output) and the EPU is determined by the needed minimum attenuation outside the passband. In Table I, $M_{i,j}$ represents the coupling coefficient between Resonator i and Resonator j. The results of analyzing the coupling matrix of Table I are shown in Fig. 2. It can be seen from Fig. 2 that loading a second-order EPU at the input or output of the

TABLE II

NORMALIZED COUPLING MATRIX OF EIGHTH-ORDER QUASI-ELLIPTIC FUNCTION FILTER WITH EQUAL RIPPLE AT THE STOPBANDS

	S	1	2	3	4	5	6	7	8	L
S	0	0	1.0406	0.8482	0	0	0	0	0	0
1	0	0	1.3421	0	0	0	0	0	0	0
2	1.0406	1.3421	0	0	0	0	0	0	0	0
3	0.8482	0	0	0	0.5984	0	0	0	0	0
4	0	0	0	0.5984	0	0.5411	0	0	0	0
5	0	0	0	0	0.5411	0	0.5915	0	0	0
6	0	0	0	0	0	0.5915	0	0	0	0.8411
7	0	0	0	0	0	0	0	0	1.6332	1.4283
8	0	0	0	0	0	0	0	1.6332	0	0
L	0	0	0	0	0	0	0.8411	1.4283	0	0

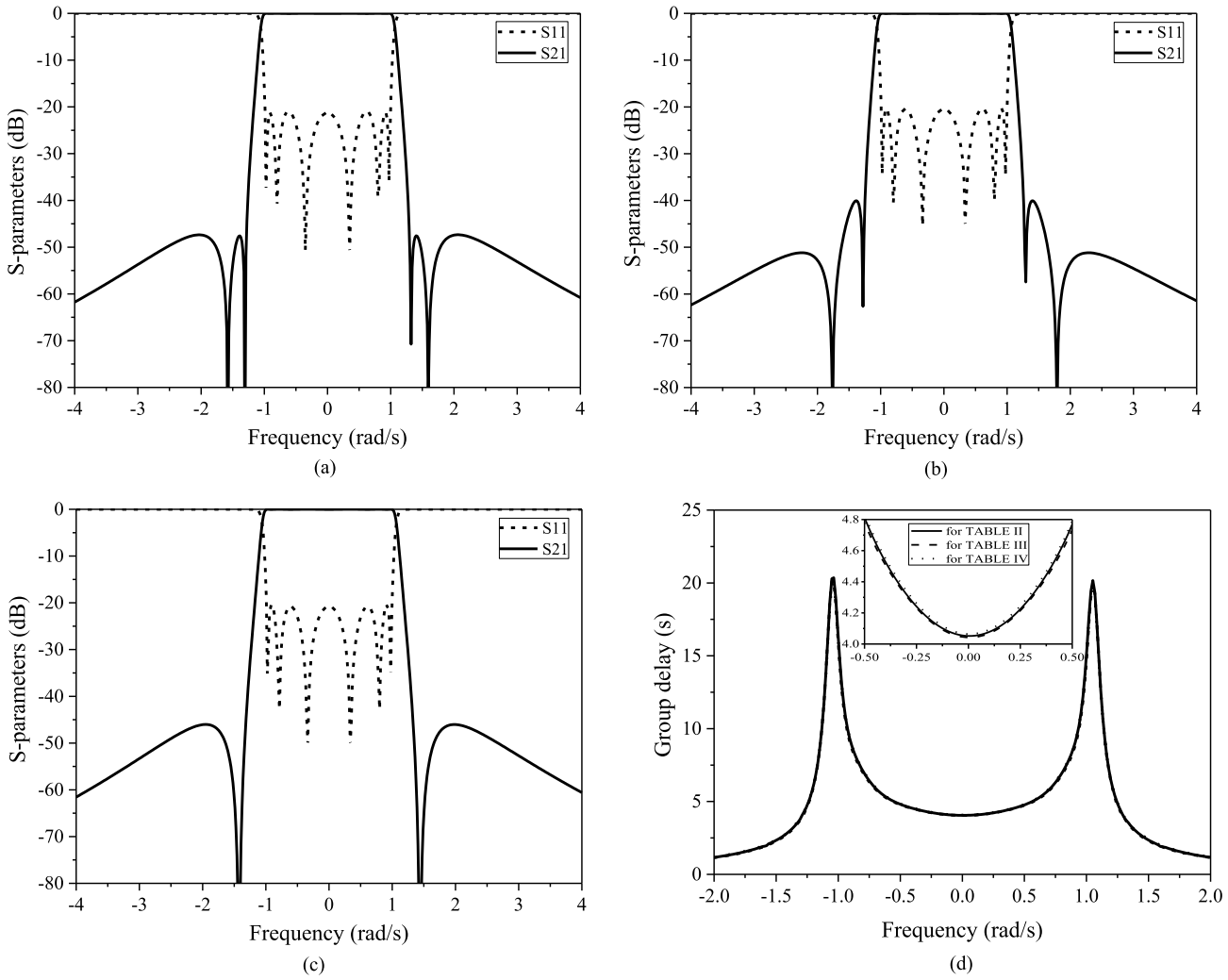

Fig. 4. Analysis of eighth-order quasi-elliptic function with two pairs of finite transmission zero coupling matrix. (a) Quasi-elliptic function filter with equal ripple at the stopbands. (b) Quasi-elliptic function filter without equal ripple at the stopbands. (c) Filter with two pairs of overlapped finite transmission zeros. (d) Group delay.

filter can achieve a filter with one pair of finite transmission zeros, and they are symmetrically distributed about the center frequency of the filter.

On the basis of above sixth-order quasi-elliptic function filter with two finite transmission zeros, by loading another EPU at the other port of the filter, an eighth-order filter topology structure with two pairs of finite transmission zeros shown in Fig. 3 can be constructed. And its optimization-based synthesized normalized coupling matrix is shown in Table II. The results of analyzing the coupling matrix of Table II are shown in Fig. 4(a). It can be seen from Fig. 4(a), the filter has two pairs of finite transmission zeros, which are symmetrically situated about the center frequency of the filter. By appropriately adjusting $M_{1,2}$ and $M_{7,8}$ in Table II, a quasi-elliptic function filter without equal ripple at the stopbands can also be configured. Its normalized matrix parameters are listed

TABLE III
NORMALIZED COUPLING MATRIX OF EIGHTH-ORDER QUASI-ELLIPTIC FUNCTION FILTER WITHOUT EQUAL RIPPLE AT THE STOPBANDS

	S	1	2	3	4	5	6	7	8	L
S	0	0	1.5945	0.8335	0	0	0	0	0	0
1	0	0	1.7540	0	0	0	0	0	0	0
2	1.5945	1.7540	0	0	0	0	0	0	0	0
3	0.8335	0	0	0	0.5952	0	0	0	0	0
4	0	0	0	0.5952	0	0.5521	0	0	0	0
5	0	0	0	0	0.5521	0	0.6059	0	0	0
6	0	0	0	0	0	0.6059	0	0	0	0.8620
7	0	0	0	0	0	0	0	0	1.2710	0.9892
8	0	0	0	0	0	0	0	1.2710	0	0
L	0	0	0	0	0	0	0.8620	0.9892	0	0

TABLE IV
NORMALIZED COUPLING MATRIX OF EIGHTH-ORDER QUASI-ELLIPTIC FUNCTION FILTER WITH SYMMETRICAL STRUCTURE

	S	1	2	3	4	5	6	7	8	L
S	0	0	1.2041	0.8463	0	0	0	0	0	0
1	0	0	1.4162	0	0	0	0	0	0	0
2	1.2041	1.4162	0	0	0	0	0	0	0	0
3	0.8463	0	0	0	0.5982	0	0	0	0	0
4	0	0	0	0.5982	0	0.5479	0	0	0	0
5	0	0	0	0	0.5479	0	0.5982	0	0	0
6	0	0	0	0	0	0.5982	0	0	0	0.8463
7	0	0	0	0	0	0	0	0	1.4162	1.2041
8	0	0	0	0	0	0	0	1.4162	0	0
L	0	0	0	0	0	0	0.8463	1.2041	0	0

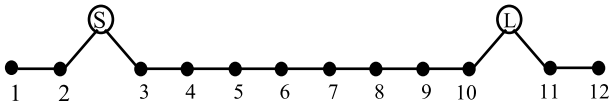

Fig. 5. Topology structure of 12th-order quasi-elliptic function filter with two pairs of finite transmission zeros.

in Table III, and the analysis of this coupling matrix is shown in Fig. 4(b). When $M_{1,2}$ is equal to $M_{7,8}$, the two pairs of finite transmission zeros can be overlapped, so symmetrical design of the filter circuit can be realized. The normalized matrix parameters are shown in Table IV, and the analysis of the coupling matrix of Table IV is depicted in Fig. 4(c). Besides, almost identical group delays for Tables II–IV can be observed from Fig. 4(d).

Based on the above simulated analysis, it has been proved that by adjusting the positions of all finite transmission zeros of the filter, the quasi-elliptic function filter with or without equal ripple at the stopband can be achieved. Moreover, the filter circuit structure can be symmetrical or asymmetrical.

Further simulations show that the finite transmission zeros can be introduced into the filter by the same method, regardless of the order of the filter. For example, according to the 12th-order filter topology shown in Fig. 5, the normalized coupling matrix presented in Table V can be synthesized. The results of analyzing the coupling matrix of Table V are shown in Fig. 6.

III. CONTROL OF FINITE TRANSMISSION ZEROS IN PRACTICAL FILTER

With using $M_{1,2}$ in Table I, making the resonant frequencies of the resonators be equal to the center frequency of the

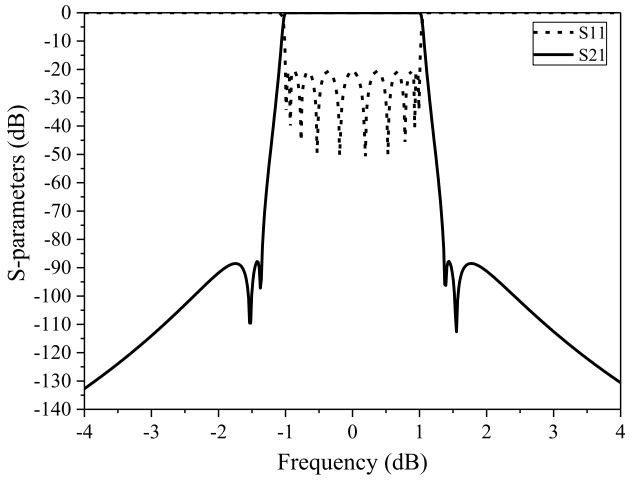

Fig. 6. Analysis of 12th-order filter prototype with two pairs of finite transmission zeros coupling matrix.

filter (2500 MHz), the simulated results of simulating the coupling between Resonator 1 and Resonator 2 in Fig. 1(b) separately are shown in Fig. 7(a) in dashed line. For comparing conveniently, the S_{21} curve in Fig. 2(a) is also depicted in Fig. 7(a). From Fig. 7(a), it can be observed that the positions of the finite transmission zeros are just the same with the resonant frequencies generated when Resonator 1 and Resonator 2 in EPUs are coupled, which is the principle of producing this type of finite transmission zeros. Thus, adjusting the coupling strength between Resonator 1 and Resonator 2 can change the relative distance between the two finite transmission zeros of the filter. Fig. 7(b) presents the relationship between the position changes of the finite

TABLE V
NORMALIZED COUPLING MATRIX OF 12TH-ORDER QUASI-ELLIPTIC FUNCTION FILTER WITH TWO PAIRS OF FINITE TRANSMISSION ZEROS

	S	1	2	3	4	5	6	7	8	9	10	11	12	L
S	0	0	1.1764	0.8443	0	0	0	0	0	0	0	0	0	0
1	0	0	1.4100	0	0	0	0	0	0	0	0	0	0	0
2	1.1764	1.4100	0	0	0	0	0	0	0	0	0	0	0	0
3	0.8443	0	0	0	0.5926	0	0	0	0	0	0	0	0	0
4	0	0	0	0.5926	0	0.5355	0	0	0	0	0	0	0	0
5	0	0	0	0	0.5355	0	0.5259	0	0	0	0	0	0	0
6	0	0	0	0	0	0.5259	0	0.5205	0	0	0	0	0	0
7	0	0	0	0	0	0	0.5205	0	0.5258	0	0	0	0	0
8	0	0	0	0	0	0	0	0.5258	0	0.5360	0	0	0	0
9	0	0	0	0	0	0	0	0	0.5360	0	0.5921	0	0	0
10	0	0	0	0	0	0	0	0	0	0.5921	0	0	0	0.8441
11	0	0	0	0	0	0	0	0	0	0	0	0	1.5800	1.3275
12	0	0	0	0	0	0	0	0	0	0	0	1.5800	0	0
L	0	0	0	0	0	0	0	0	0	0	0.8441	1.3275	0	0

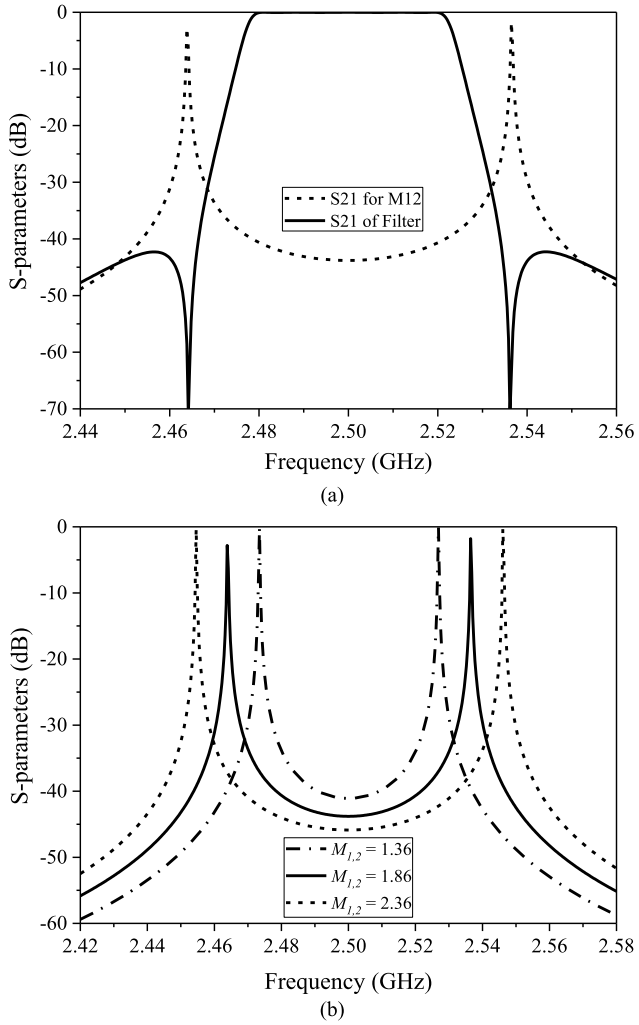

Fig. 7. Control of the finite transmission zeros. (a) Generation of the finite transmission zeros. (b) Location changes of finite transmission zeros with different $M_{1,2}$.

transmission zeros and $M_{1,2}$ in Table I. As shown in Fig. 7(b), the larger the $M_{1,2}$, the farther away from each other are the finite transmission zeros, and the smaller the $M_{1,2}$, the closer are the finite transmission zeros. And when the frequencies of the Resonator 1 and Resonator 2 are equal to the filter's center frequency, the finite transmission zeros are always symmetrically located about the center frequency of the filter.

In the above discussion, the resonant frequency of each resonator in the EPUs is the same with the center frequency of the filter. If the resonant frequency of each resonator in the EPUs is changed to make their resonant frequencies are not equal to the center frequency of the filter, the finite transmission zeros can achieve asymmetrical distribution, and even the two finite transmission zeros can be simultaneously distributed on one side outside the filter passband to meet the requirement of special steep rejection. For example, for the circuit topology shown in Fig. 1(b), Fig. 8 presents that when the frequencies of the Resonator 1 and Resonator 2 in the EPU are the same, the positions of the finite transmission zeros can be shifted by adjusting their resonant frequencies. When the resonant frequencies of Resonator 1 and Resonator 2 decrease slightly, the asymmetrical distribution of two finite transmission zeros in the filter band edges is shown in Fig. 8(a), and if their resonant frequencies move down relatively dramatically, the situation of two finite transmission zeros distributed simultaneously on lower side outside the filter passband is shown in Fig. 8(b). Their corresponding coupling matrices are listed in Tables VI and VII, respectively. On the contrary, if their resonant frequencies increase a lot, the two finite transmission zeros can be both located on the upper side, as shown in Fig. 8(c), and its coupling matrix is displayed in Table VIII. It can be thought if the resonant frequencies of Resonator 1 and Resonator 2 are set to be different values, by using asynchronous tuning technique, the adjustment of finite transmission zeros will be more flexible. In addition, if there are several pairs of finite transmission zeros, each pair of finite transmission zeros can be controlled separately.

It is worth noting that the two resonators in each EPU have been used to generate a pair of finite transmission zeros outside the passband, which leads that only one transmission pole can be produced within the passband by each EPU, so the total number of transmission poles in the passband is always equal to the quantity of the resonators in the filter's main signal path plus the number of EPUs, no matter what the filter's order is odd or even. It can be observed that all the previous theoretical S-parameter responses of the filter topologies with EPU conform to this rule, while there is no such phenomenon

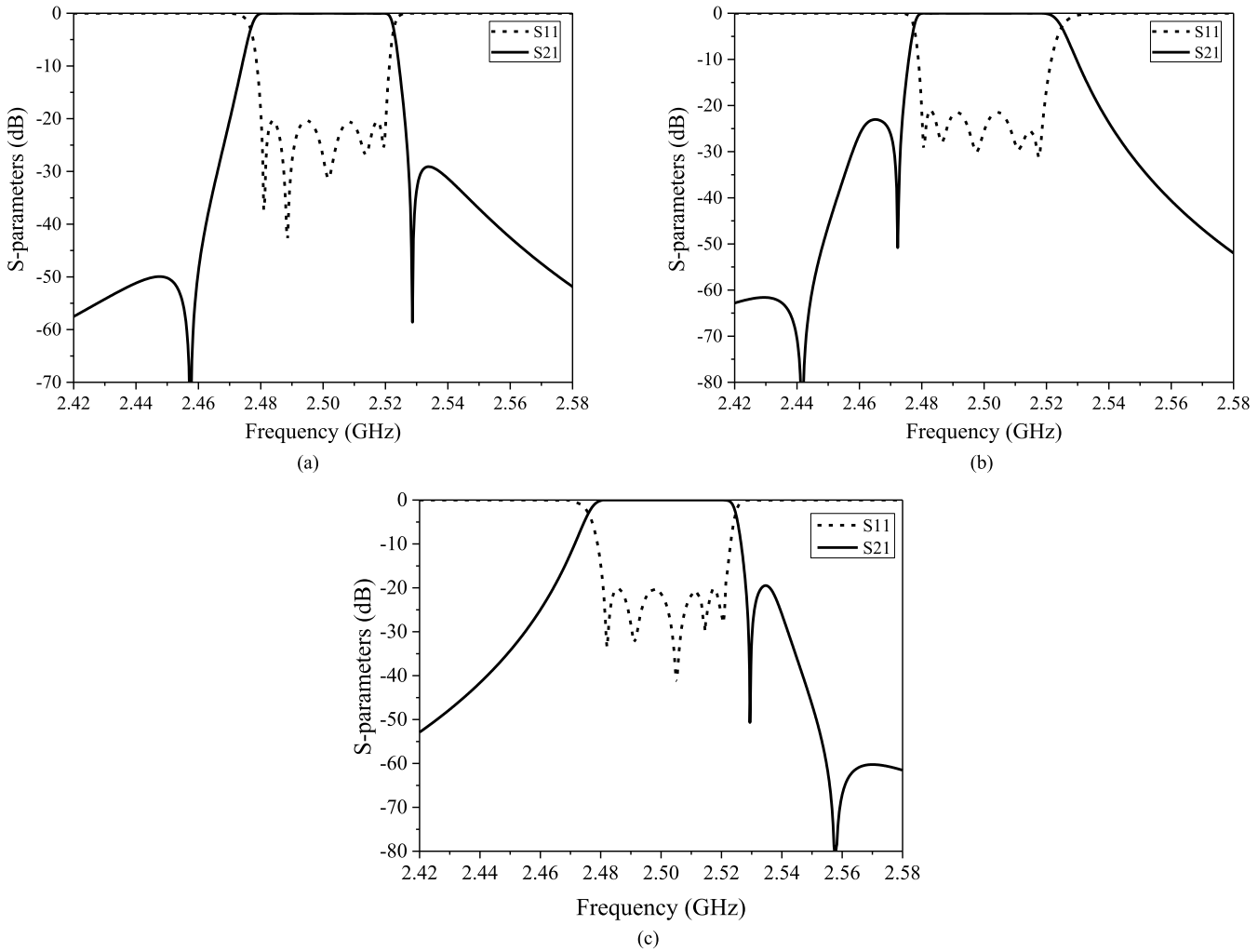

Fig. 8. Arbitrary distribution of finite transmission zeros. (a) Finite transmission zeros distributed on both band edges of the filter. (b) Finite transmission zeros located on lower side outside the filter passband. (c) Finite transmission zeros located on upper side outside the filter passband.

TABLE VI

NORMALIZED COUPLING MATRIX FOR FIG. 8(a)

	S	1	2	3	4	5	6	L
S	0	0	1.5507	0.8595	0	0	0	0
1	0	0	1.3000	0	0	0	0	0
2	1.5507	1.3000	0	0	0	0	0	0
3	0.8595	0	0	0	0.6365	0	0	0
4	0	0	0	0.6365	0	0.6311	0	0
5	0	0	0	0	0.6311	0	0.8647	0
6	0	0	0	0	0	0.8647	0	1.0278
L	0	0	0	0	0	0	1.0278	0

TABLE VII

NORMALIZED COUPLING MATRIX FOR FIG. 8(b)

	S	1	2	3	4	5	6	L
S	0	0	1.1143	0.8321	0	0	0	0
1	0	0	0.5545	0	0	0	0	0
2	1.1143	0.5545	0	0	0	0	0	0
3	0.8321	0	0	0	0.6526	0	0	0
4	0	0	0	0.6526	0	0.6109	0	0
5	0	0	0	0	0.6109	0	0.8343	0
6	0	0	0	0	0	0.8343	0	1.0112
L	0	0	0	0	0	0	1.0112	0

TABLE VIII

NORMALIZED COUPLING MATRIX FOR FIG. 8(c)

	S	1	2	3	4	5	6	L
S	0	0	1.2476	0.8692	0	0	0	0
1	0	0	0.4198	0	0	0	0	0
2	1.2476	0.4198	0	0	0	0	0	0
3	0.8692	0	0	0	0.7132	0	0	0
4	0	0	0	0.7132	0	0.6669	0	0
5	0	0	0	0	0.6669	0	0.8951	0
6	0	0	0	0	0	0.8951	0	1.0387
L	0	0	0	0	0	0	1.0387	0

in the conventional extracted-pole structure filter. In order to analyze the precise positions of the missing transmission poles, the effective Cauchy method is adopted. The famous Cauchy method can generate the rational polynomial interpolation of the passive device by sampling the simulated or measured S-parameter response of passive devices for further analysis, especially for analyzing the precise locations of reflection zeros and transmission zeros [37]. Since lots of literature has conducted a thorough study of Cauchy method, so it is briefly described here. First, for a two-port filter circuit, its response can be characterized by the scattering parameters S_{11} and S_{21}, where the reflection function S_{11} can be expressed by the ratio of two polynomials $F(s)$ and $E(s)$ with finite degrees, and polynomials $P(s)$ and $E(s)$ can define the transfer function S_{21}. The polynomial model corresponding to the filter in the normalized low-pass domain s is shown in (1), where

the complex coefficients $a_k^{(1)}$ and $a_k^{(2)}$ can be obtained by computing the over determined equation expressed as (2), and ε is a constant normalizing S_{21} to the equal-ripple level at $\omega = \pm 1$ (ω is the real frequency variable related to the more familiar complex frequency variable s by $s = j\omega$) as in (3) [36], [38]

$$S_{11}(s) = \frac{F(s)}{E(s)} = \frac{\sum_{k=0}^{n} a_k^{(1)} s^k}{\sum_{k=0}^{n} b_k s^k}$$

$$S_{21}(s) = \frac{P(s)}{\varepsilon E(s)} = \frac{\sum_{k=0}^{nz} a_k^{(2)} s^k}{\varepsilon \sum_{k=0}^{n} b_k s^k} \tag{1}$$

$$\left[S_{21}V_n - S_{11}V_{nz}\right]\begin{bmatrix} a^{(1)} \\ a^{(2)} \end{bmatrix} = X\begin{bmatrix} a^{(1)} \\ a^{(2)} \end{bmatrix} = 0 \tag{2}$$

$$\varepsilon = \frac{1}{\sqrt{10^{RL/10} - 1}} \cdot \left.\frac{P(s)}{F(s)}\right|_{s=j} \tag{3}$$

where

$$a^{(1)} = \left[a_n^{(1)}, a_{n-1}^{(1)}, \ldots, a_0^{(1)}\right]^T$$
$$a^{(2)} = \left[a_{nz}^{(2)}, a_{nz-1}^{(2)}, \ldots, a_0^{(2)}\right]^T$$
$$S_{11} = \text{diag}\left\{S_{11}(s_i)\right\}_{i=1,\ldots,N}$$
$$S_{21} = \text{diag}\left\{S_{21}(s_i)\right\}_{i=1,\ldots,N}.$$

And V_{r} is a Vandermonde matrix defined as

$$V_r = \begin{bmatrix} 1 & s_1 & s_1^2 & \cdots & s_1^r \\ 1 & s_2 & s_2^2 & \cdots & s_2^r \\ \vdots & \vdots & \vdots & \ddots & \vdots \\ 1 & s_N & s_N^2 & \cdots & s_N^r \end{bmatrix}. \tag{4}$$

N is the number of sampling points for the simulated or measured S-parameter response, and the normalized frequency of the corresponding sampling point is $s_i = j\omega_i$ obtained from a bandpass to low-pass transformation. n is the filter order, and nz is the number of transmission zeros at finite complex frequencies. Note that N should be greater than or equal to $n+nz+1$, and all of the frequency points used in the generation of the rational polynomial model must be chosen in or near the passband [39], and it is best to include the reflection zeros and transmission zeros. The total least-squares (TLS) method and singular value decomposition are used to solve the following over determined system [38]:

$$X\begin{bmatrix} a^{(1)} \\ a^{(2)} \end{bmatrix} = U\Sigma V^H \begin{bmatrix} a^{(1)} \\ a^{(2)} \end{bmatrix} = 0 \tag{5}$$

where U and V are unitary matrices and Σ is a diagonal matrix of the ordered singular values of X, and $(\cdot)^H$ represents the complex conjugate transpose matrix. The last column of the unitary matrix V^H is proportional to the optimum solution ($a_k^{(1)}$ and $a_k^{(2)}$). So polynomials $F(s)$ and $P(s)$ are determined now. Subsequently, according to the energy conservation equation shown in the following equation, the common denominator $E(s)$ in (1) can be derived

$$F(s)F^*(-s) + P(s)P^*(-s)/\varepsilon^2 = E(s)E^*(-s). \tag{6}$$

For the stability of the filter, the n roots of $E(s)E^*(-s)$ located in the left half of the complex plane s are selected as roots of $E(s)$ [39]. Then, coefficients b_{k} can be eventually determined from the poles.

Based on the above theory of the Cauchy method, the locations of the transmission poles and transmission zeros of the filter can be accurately calculated according to the rational polynomial interpolation. Here, the eighth-order filter with coupling matrix shown in Table III is taken as an example to analyze the locations of transmission poles and transmission zeros. The filter's simulated S-parameter response is sampled, and the samples are brought into a MATLAB parameter extraction program based on the Cauchy method. The coefficients of polynomials $F(s)$, $P(s)$, and $E(s)$ are calculated, as shown in Table IX. Then, the precise locations of transmission poles and transmission zeros can be determined from the roots of $F(s)$ and $P(s)$, respectively, as presented in Table X, where it can be observed that there are six transmission poles situated at real frequencies (on the imaginary axis of the complex plane), and the remaining two are placed on the complex plane with a real part different from zero. This is the reason why only six transmission poles can be seen in the passband of the S-parameter response curve. Similarly, the EPU configuration filters with other orders can use the same analytic approach to calculate their rational polynomial model and analyze the locations of their transmission poles and transmission zeros.

In terms of the passband selectivity, the proposed EPU configuration filter is indeed slightly inferior to that of the

TABLE IX

EIGHT-DEGREE FILTER WITH TWO PAIRS OF FINITE TRANSMISSION ZEROS: COEFFICIENTS OF TRANSFER AND REFLECTION POLYNOMIALS $RL = 20$ dB, $\varepsilon = 0.7931$

s^n	Polynomial Coefficients		
$n =$	$F(s)$	$P(s)$	$E(s)$
8	1.0000	0.0000	1.0000
7	-1.7751 + 0.0020j	0.0000	5.5051 + 0.0020j
6	-0.2613 + 0.0008j	0.0000	13.3164 + 0.0068j
5	-2.8416 + 0.0026j	0.0000	22.5130 + 0.0137j
4	-2.5932 + 0.0016j	-0.0002 - 0.3079j	27.6704 + 0.0192j
3	-1.1215 + 0.0009j	0.0000	25.2451 + 0.0192j
2	-1.5322 + 0.0008j	-0.0008 - 1.4786j	17.0413 + 0.0140j
1	-0.0293	0.0000	7.8091 + 0.0068j
0	-0.1526 + 0.0001j	-0.0009 - 1.6004j	2.0237 + 0.0019j

TABLE X

SINGULARITIES OF EIGHT-DEGREE EPU CONFIGURATION FILTER WITH TWO PAIRS OF FINITE TRANSMISSION ZEROS

	Reflection Zeros (Roots of $F(s)$)	Transmission Zeros (Roots of $P(s)$)
1	-0.0032 - 0.9763j	-1.7757j
2	0.0099 - 0.7966j	-1.2836j
3	0.0350 - 0.3440j	1.2838j
4	0.0350 + 0.3440j	1.7760j
5	0.0099 + 0.7966j	
6	-0.0033 + 0.9761j	
7	-0.8351 - 0.0001j	
8	2.5269 - 0.0018j	

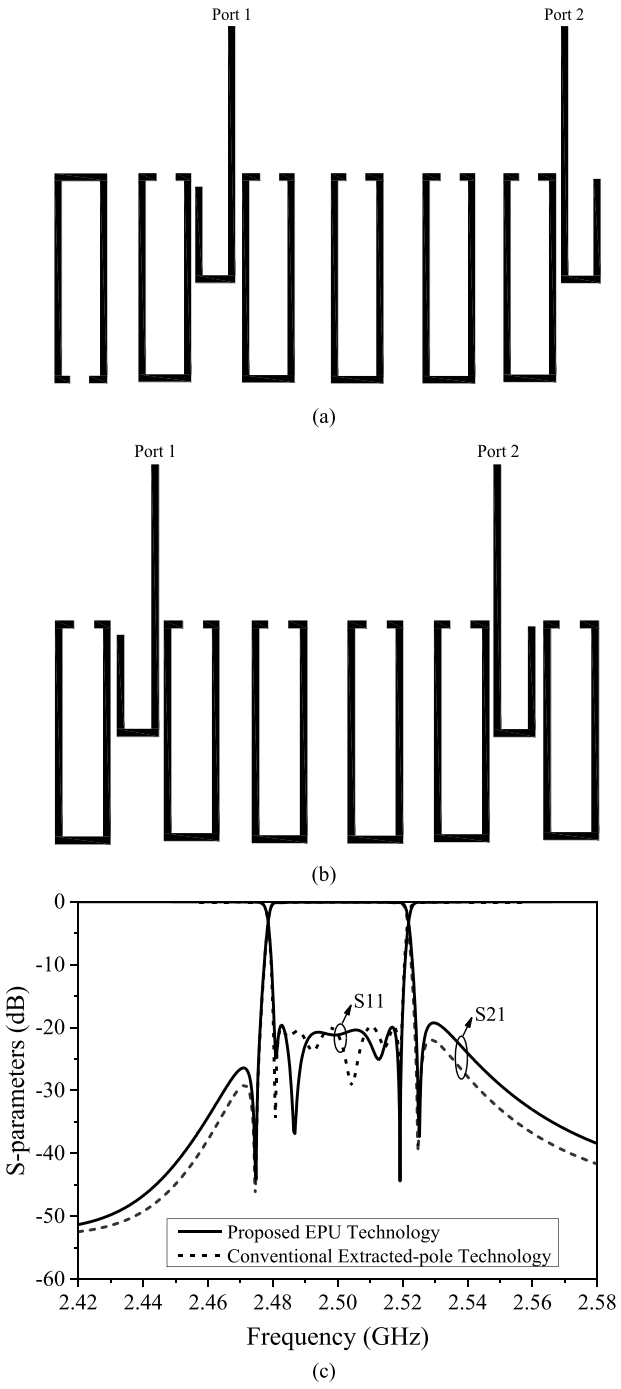

Fig. 9. (a) Filter with proposed EPU technology. (b) Filter with conventional extracted-pole technology. (c) Simulated responses.

traditional extracted-pole filter with the same order because of the missing transmission poles situated on complex plane with a real part different from zero. However, when two pairs of finite transmission zeros are needed, the filter loaded with EPU is more likely to realize a miniaturized structure compared with the conventional extracted-pole filter. Because by adding one EPU at the input and output, respectively, two pairs of finite transmission zeros can be generated, while using the extracted-pole technique to create two pairs of finite transmission zeros, in addition to the need for four

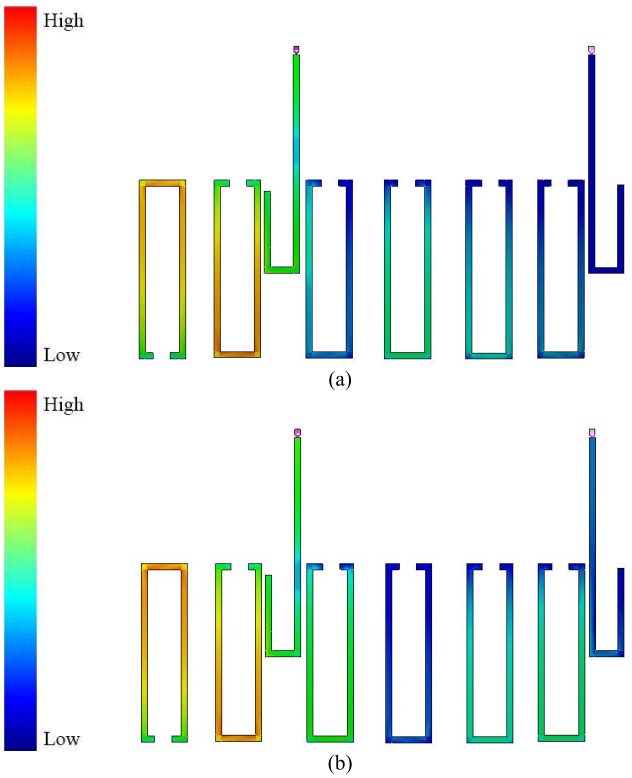

Fig. 10. (a) Simulated current density distributions of the filter with proposed EPU technology at f_{TZ1}. (b) At f_{TZ2}.

dedicated resonators, multiple phase shifters are also needed. Besides, the frequencies of resonators in EPU are the same as the central frequency of the filter, which means that it is more convenient to adjust the filter's center frequency through changing the frequencies of all resonators by equal proportions. However, the frequencies of the dedicated resonators are equal to those of the introduced finite transmission zeros in the extracted-pole technique.

IV. Analysis of Current Density Distribution

To show the differences between the proposed EPU technology and conventional extracted-pole one, their current density distributions are analyzed in this section. Fig. 9(a) and (b) shows the filter with proposed EPU technology and the filter with conventional extracted-pole technology, respectively. And their simulated responses are illustrated in Fig. 9(c), where these two filters shows similar performance, especially the same locations of two finite transmission zeros (f_{TZ1} and f_{TZ2}).

Fig. 10(a) and (b) depicts the current distributions of the filter with proposed EPU technology at the frequencies of two finite transmission zeros f_{TZ1} and f_{TZ2}, respectively, when voltage source is fed into Port 1 with Port 2 as the output port. It is shown that the current is mainly concentrated on the EPU at both f_{TZ1} and f_{TZ2}, which causes the simultaneous generation of two finite transmission zeros.

Fig. 11(a) and (b) depicts the current distributions along the filter with conventional extracted-pole technology under the same frequencies of two finite transmission

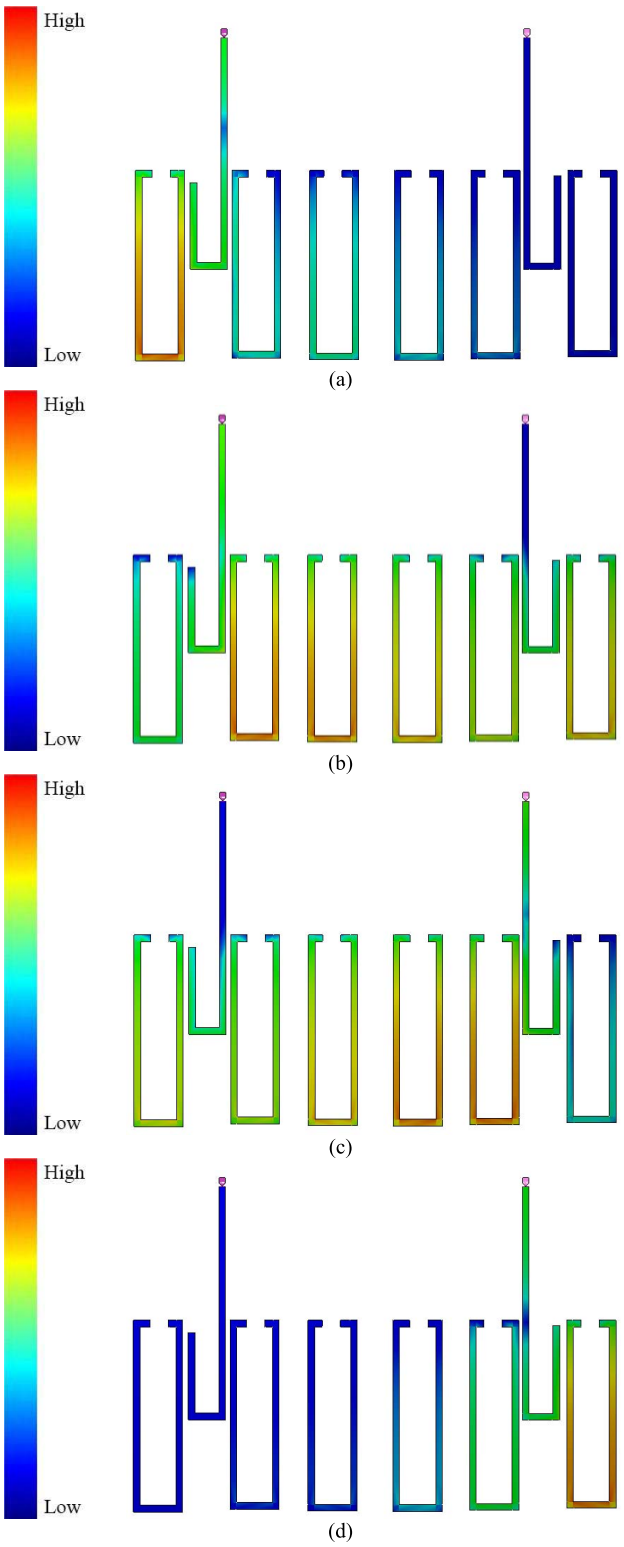

Fig. 11. (a) Simulated current density distributions of the filter with conventional extracted-pole technology at f_{TZ1} with Port 1 fed by voltage source. (b) At f_{TZ2} with Port 1 fed by voltage source. (c) Simulated current density distributions of the filter with conventional extracted-pole technology at f_{TZ1} with Port 2 fed by voltage source. (d) At f_{TZ2} with Port 2 fed by voltage source.

zeros f_{TZ1} and f_{TZ2}, respectively, when Port 1 is fed by voltage source with Port 2 as the output port. It is obviously found that the current is mainly concentrated on the left dedicated resonator with the frequency of the voltage source equal to its resonant frequency f_{TZ1}, and when the frequency of the voltage source equal to the right dedicated resonator's resonant frequency f_{TZ2}, the current moves to the right of the filter. Similarly, through analyzing Fig. 11(c) and (d), when Port 2 is fed by voltage source with Port 1 as the output port, a similar phenomenon will occur on the right dedicated resonator. The current distribution results of Fig. 11(a)–(d) mean that the left and right dedicated resonators are responsible for the generation of the left and right finite transmission zeros f_{TZ1} and f_{TZ2}, respectively. Thus, for the filter with conventional

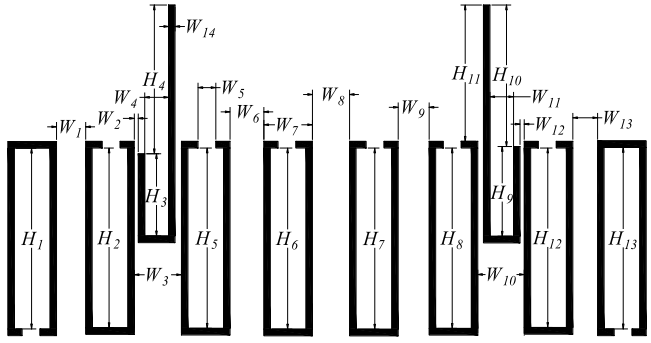

Fig. 12. Layout of eighth-order quasi-elliptic function HTS filter circuit with two pairs of finite transmission zeros. (Dimensions: $W_1 = 1.125$, $W_2 = 0.152$, $W_3 = 1.818$, $W_4 = 0.919$, $W_5 = 0.687$, $W_6 = 1.305$, $W_7 = 1.874$, $W_8 = 1.432$, $W_9 = 1.195$, $W_{10} = 1.792$, $W_{11} = 0.911$, $W_{12} = 0.162$, $W_{13} = 0.956$, $W_{14} = 0.250$, $H_1 = 6.693$, $H_2 = 6.654$, $H_3 = 3.043$, $H_4 = 5.512$, $H_5 = 6.678$, $H_6 = 6.708$, $H_7 = 6.712$, $H_8 = 6.681$, $H_9 = 3.323$, $H_{10} = 5.243$, $H_{11} = 5.050$, $H_{12} = 6.648$, $H_{13} = 6.723$, all in millimeters).

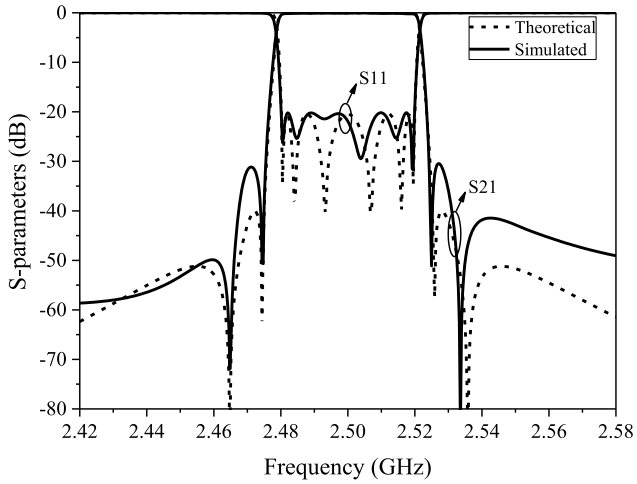

Fig. 13. Simulated and theoretical frequency response curves of the HTS filter.

Fig. 14. Photograph of the fabricated HTS filter.

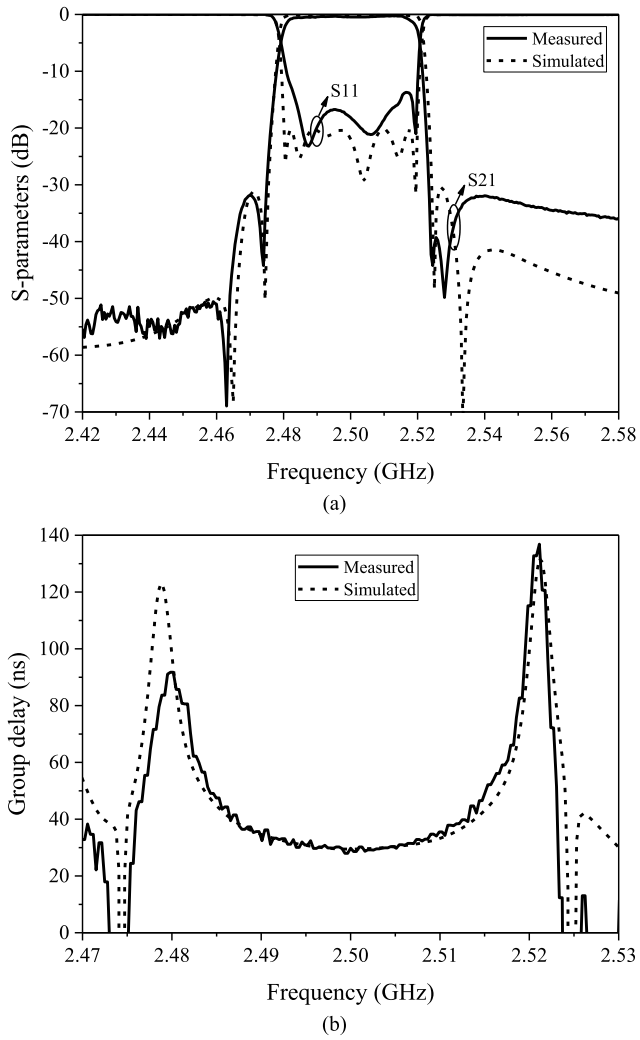

Fig. 15. Measured and simulated results of the HTS filter. (a) S-parameters. (b) Group delay.

extracted-pole technology, one dedicated resonator can only produce one finite transmission zero situated at the resonant frequency of the dedicated resonator, while for the filter with proposed EPU technology, a pair of finite transmission zeros can be generated simultaneously by loading an EPU, and they are located at the resonant frequencies separated from the two mutual coupled resonators in the EPU.

V. Design of Eighth-Order HTS Filter With Two Pairs of Finite Transmission Zeros Using EPU Technology

In order to make the simulated results approximate the theoretical results for verifying the feasibility of the proposed method, the high-temperature superconducting (HTS) thin film is adopted to design the actual circuit, mainly because the HTS film has a very low microwave surface resistance and the filters designed on it possess an extremely high Q value [41]–[47]. Then, an eighth-order HTS filter is designed on the double-sided YBCO/$LaAlO_3$/YBCO HTS thin film with the size of 24.6 mm $\times$ 12.2 mm, the thickness of 0.5 mm, and the dielectric constant of 24 by using the coupling matrix in Table III. The layout of this filter circuit is shown in Fig. 12. As it shown, the circuit possesses a conventional simple single-row filter structure without any cross-coupling, and the method of coupled-line coupling is used to all of the external couplings to minimize the size of the circuit. Furthermore, ordinary resonator's structures can be used to achieve this kind of design. The frequency response curve shown in Fig. 13 is obtained by using the full-wave simulation software. It can be seen from Fig. 13 that the simulated curves of amplitude frequency are consistent with the theoretical ones, which means that the optimization-based synthesized coupling matrix can be completely realized by actual circuit.

Fig. 14 shows the photograph of the fabricated filter. Fig. 15 shows the simulated and measured results of the HTS filter at the temperature of 72.5 K. The measured results show that the center frequency of the filter is 2500 MHz; the bandwidth is 40 MHz; the reflection in the passband is better than -13.2 dB; and the insertion loss at the center frequency is 0.35 dB. So the measured results agree rather well with the simulated ones. This also proves that the quasi-elliptic function filter topology shown in Fig. 3 can be completely used for the filter design and fabrication. Therefore, the feasibility of the new design method of producing finite transmission zeros on the filter band edges is verified.

VI. Conclusion

A pair of coupled resonators is used to construct a new second-order EPU that can be loaded at the input or output of a filter for introducing even finite transmission zeros. These finite transmission zeros can be located on both sides outside the filter passband about the filter's center frequency symmetrically or asymmetrically, even entirely on one side. Though this method, the quasi-elliptic function filter with multiple finite transmission zeros can be achieved without any cross-coupling. And the proposed method is verified by designing an eighth-order HTS filter, which can provide reference for the design of high-order filter circuit.

References

[1] L. Athukorala and D. Budimir, "Design of compact dual-mode microstrip filters," *IEEE Trans. Microw. Theory Techn.*, vol. 58, no. 11, pp. 2888–2895, Nov. 2010.

[2] X.-H. Wu, Q.-X. Chu, and L.-L. Qiu, "Differential wideband bandpass filter with high-selectivity and common-mode suppression," *IEEE Microw. Wireless Compon. Lett.*, vol. 23, no. 12, pp. 644–646, Dec. 2013.

[3] R. Levy, "Filters with single transmission zeros at real or imaginary frequencies," *IEEE Trans. Microw. Theory Techn.*, vol. MTT-24, no. 4, pp. 172–181, Apr. 1976.

[4] T. Yan, D. Lu, J. Wang, and X.-H. Tang, "High-selectivity balanced bandpass filter with mixed electric and magnetic coupling," *IEEE Microw. Wireless Compon. Lett.*, vol. 26, no. 6, pp. 398–400, Jun. 2016.

[5] A. Corona-Chavez, M. J. Lancaster, and H. T. Su, "HTS quasi-elliptic filter using capacitive-loaded cross-shape resonators with low sensitivity to substrate thickness," *IEEE Trans. Microw. Theory Techn.*, vol. 55, no. 1, pp. 117–120, Jan. 2007.

[6] G. Zhang, F. Huang, and M. J. Lancaster, "Superconducting spiral filters with quasi-elliptic characteristic for radio astronomy," *IEEE Trans. Microw. Theory Techn.*, vol. 53, no. 3, pp. 947–951, Mar. 2005.

[7] S. M. I. Tsuzuki, S. Ye, and S. Berkowitz, "Ultra-selective 22-pole 10-transmission zero superconducting bandpass filter surpasses 50-pole Chebyshev filter," *IEEE Trans. Microw. Theory Techn.*, vol. 50, no. 12, pp. 2924–2929, Dec. 2002.

[8] A. B. Jayyousi and M. J. Lancaster, "A gradient-based optimization technique employing determinants for the synthesis of microwave coupled filters," in *IEEE MTT-S Int. Microw. Symp. Dig.*, Jun. 2004, vol. 3, no. 3, pp. 1369–1372.

[9] G. Macchiarella, "Accurate synthesis of inline prototype filters using cascaded triplet and quadruplet sections," *IEEE Trans. Microw. Theory Techn.*, vol. 50, no. 7, pp. 1779–1783, Jul. 2002.

[10] S. Amari, U. Rosenberg, and J. Bornemann, "Adaptive synthesis and design of resonator filters with source/load-multiresonator coupling," *IEEE Trans. Microw. Theory Techn.*, vol. 50, no. 8, pp. 1969–1978, Aug. 2002.

[11] R. N. Gajaweera and L. F. Lind, "Coupling matrix extraction for cascaded-triplet (CT) topology," *IEEE Trans. Microw. Theory Techn.*, vol. 52, no. 3, pp. 768–772, Mar. 2004.

[12] J.-S. Hong and M. J. Lancaster, "Couplings of microstrip square open-loop resonators for cross-coupled planar microwave filters," *IEEE Trans. Microw. Theory Techn.*, vol. 44, no. 11, pp. 2099–2109, Nov. 1996.

[13] B.-C. Min, Y. H. Choi, S. K. Kim, and B. Oh, "Cross-coupled band-pass filter using HTS microstrip resonators," *IEEE Trans. Appl. Supercond.*, vol. 11, no. 1, pp. 485–488, Mar. 2001.

[14] J.-S. Hong and M. J. Lancaster, "Design of highly selective microstrip bandpass filters with a single pair of attenuation poles at finite frequencies," *IEEE Trans. Microw. Theory Techn.*, vol. 48, no. 7, pp. 1098–1107, Jul. 2000.

[15] A. Lamecki, P. Kozakowski, and M. Mrozowski, "Fast synthesis of coupled-resonator filters," *IEEE Microw. Wireless Compon. Lett.*, vol. 14, no. 4, pp. 174–176, Apr. 2004.

[16] C.-C. Yang and C.-Y. Chang, "Microstrip cascade trisection filter," *IEEE Microw. Guided Wave Lett.*, vol. 9, no. 7, pp. 271–273, Jul. 1999.

[17] A. E. Atia and A. E. Williams, "Narrow-bandpass waveguide filters," *IEEE Trans. Microw. Theory Techn.*, vol. MTT-20, no. 4, pp. 258–265, Apr. 1972.

[18] R. Levy, "New cascaded trisections with resonant cross-couplings (CTR sections) applied to the design of optimal filters," in *IEEE MTT-S Int. Microw. Symp. Dig.*, vol. 2, Jun. 2004, pp. 447–450.

[19] J.-S. Hong, M. J. Lancaster, D. Jedamzik, R. B. Greed, and J. C. Mage, "On the performance of HTS microstrip quasi-elliptic function filters for mobile communications application," *IEEE Trans. Microw. Theory Techn.*, vol. 48, no. 7, pp. 1240–1246, Jul. 2000.

[20] R. N. Gajaweera and L. F. Lind, "Rapid coupling matrix reduction for longitudinal and cascaded-quadruplet microwave filters," *IEEE Trans. Microw. Theory Techn.*, vol. 51, no. 5, pp. 1578–1583, May 2003.

[21] S. Amari, U. Rosenberg, and J. Bornemann, "Singlets, cascaded singlets, and the nonresonating node model for advanced modular design of elliptic filters," *IEEE Microw. Wireless Compon. Lett.*, vol. 14, no. 5, pp. 237–239, May 2004.

[22] R. J. Cameron, A. R. Harish, and C. J. Radcliffe, "Synthesis of advanced microwave filters without diagonal cross-couplings," *IEEE Trans. Microw. Theory Techn.*, vol. 50, no. 12, pp. 2862–2872, Dec. 2002.

[23] L. Gao *et al.*, "8-GHz narrowband high-temperature superconducting filter with high selectivity and flat group delay," *IEEE Trans. Microw. Theory Techn.*, vol. 57, no. 7, pp. 1767–1773, Jul. 2009.

[24] G. Zhang, M. J. Lancaster, and F. Huang, "A high-temperature superconducting bandpass filter with microstrip quarter-wavelength spiral resonators," *IEEE Trans. Microw. Theory Techn.*, vol. 54, no. 2, pp. 559–563, Feb. 2006.

[25] J.-S. Hong, E. P. McErlean, and B. Karyamapudi, "High-order superconducting filter with group delay equalization," in *IEEE MTT-S Int. Microw. Symp. Dig.*, Jun. 2005, pp. 1467–1470.

[26] J. Zhou, M. J. Lancaster, F. Huang, N. Roddis, and D. Glynn, "HTS narrow band filters at UHF band for radio astronomy applications," *IEEE Trans. Appl. Supercond.*, vol. 15, no. 2, pp. 1004–1007, Jun. 2005.

[27] T. Zhang *et al.*, "Miniaturized HTS linear phase filter based on neighboring CQ units sharing resonators," *Superconductor Sci. Technol.*, vol. 28, no. 10, p. 105012, Sep. 2015.

[28] J.-S. Hong, E. P. McErlean, and B. Karyamapudi, "Narrowband high temperature superconducting filter for mobile communication systems," *IEE Proc.-Microw., Antennas Propag.*, vol. 151, no. 6, pp. 491–496, Dec. 2004.

[29] J.-S. Hong and E. P. McErlean, "Narrow-band HTS filter on sapphire substrate," in *IEEE MTT-S Int. Microw. Symp. Dig.*, Jun. 2004, pp. 1105–1108.

[30] Y. Yang, M. Yu, and Q. Wu, "Advanced synthesis technique for extracted pole and NRN filters," in *IEEE MTT-S Int. Microw. Symp. Dig.*, May 2016, pp. 1–4.

[31] Y. Yang, M. Yu, and Q. Wu, "Advanced synthesis technique for unified extracted pole filters," *IEEE Trans. Microw. Theory Techn.*, vol. 64, no. 12, pp. 4463–4472, Dec. 2016.

[32] Y. He, G. Wang, and L. Sun, "Direct matrix synthesis approach for narrowband mixed topology filters," *IEEE Microw. Wireless Compon. Lett.*, vol. 26, no. 5, pp. 301–303, May 2016.

[33] J. D. Rhodes and R. J. Cameron, "General extracted pole synthesis technique with applications to low-loss TE_{011} mode filters," *IEEE Trans. Microw. Theory Techn.*, vol. MI-28, no. 9, pp. 1018–1028, Sep. 1980.

[34] J. R. Montejo-Garai, J. A. Ruiz-Cruz, J. M. Rebollar, M. J. Padilla-Cruz, A. Onoro-Navarro, and I. Hidalgo-Carpintero, "Synthesis and design of in-line N-order filters with N real transmission zeros by means of extracted poles implemented in low-cost rectangular H-plane waveguide," *IEEE Trans. Microw. Theory Techn.*, vol. 53, no. 5, pp. 1636–1642, May 2005.

[35] K. S. K. Yeo and M. J. Lancaster, "The design of microstrip six-pole quasi-elliptic filter with linear phase response using extracted-pole technique," *IEEE Trans. Microw. Theory Techn.*, vol. 49, no. 2, pp. 321–327, Feb. 2001.

[36] R. J. Cameron, "General coupling matrix synthesis methods for Chebyshev filtering functions," *IEEE Trans. Microw. Theory Techn.*, vol. 47, no. 4, pp. 433–442, Apr. 1999.

[37] R. S. Adve, T. K. Sarkar, S. M. Rao, E. K. Miller, and D. R. Pflug, "Application of the Cauchy method for extrapolating/interpolating narrowband system responses," *IEEE Trans. Microw. Theory Techn.*, vol. 45, no. 5, pp. 837–845, May 1997.

[38] G. Macchiarella and D. Traina, "A formulation of the Cauchy method suitable for the synthesis of lossless circuit models of microwave filters from lossy measurements," *IEEE Microw. Wireless Compon. Lett.*, vol. 16, no. 5, pp. 243–245, May 2006.

[39] A. García-Lampérez, S. Llorente-Romano, M. Salazar-Palma, and T. K. Sarkar, "Efficient electromagnetic optimization of microwave filters and multiplexers using rational models," *IEEE Trans. Microw. Theory Techn.*, vol. 52, no. 2, pp. 508–521, Feb. 2004.

[40] A. Saito *et al.*, "Design and performance of transmit filters using HTS bulk resonators for IMT-advanced applications," *IEEE Trans. Appl. Supercond.*, vol. 17, no. 2, pp. 886–889, Jun. 2007.

[41] N. Sekiya, "Design of highâŁ"order HTS dualâŁ"band bandpass filters with receiver subsystem for future mobile communication systems," *Phys. C, Supercond. Appl.*, vol. 527, pp. 91–97, Aug. 2016.

[42] H. Liu, P. Wen, S. Zhu, B. Ren, and Y. He, "High-temperature superconducting composite right/left-handed resonator," *IEEE Trans. Appl. Supercond.*, vol. 26, no. 3, Apr. 2016, Art. no. 1500204.

[43] L. Sun and Y. He, "Research progress of high temperature superconducting filters in china," *IEEE Trans. Appl. Supercond.*, vol. 24, no. 5, Oct. 2014, Art. no. 1501308.

[44] X. Lu *et al.*, "Superconducting ultra-wideband (UWB) bandpass filter design based on quintuple/quadruple/ triple-mode resonator," *IEEE Trans. Microw. Theory Techn.*, vol. 63, no. 4, pp. 1281–1293, Apr. 2015.

[45] K. Satoh, T. Mimura, S. Narahashi, and T. Nojima, "The 2 GHz high temperature superconducting receiver equipment for mobile communications," *Phys. C, Supercond.*, vols. 357–360, pp. 1495–1502, Aug. 2001.

[46] H. Liu, P. Wen, H. Jiang, and Y. He, "Wideband and low-loss high-temperature superconducting bandpass filter based on metamaterial stepped-impedance resonator," *IEEE Trans. Appl. Supercond.*, vol. 26, no. 3, Apr. 2016, Art. no. 1500404.

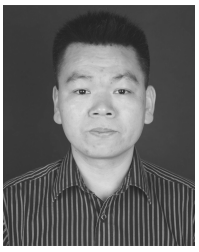

Tianliang Zhang (M'15) was born in 1976. He received the M.S. and Ph.D. degrees in physical electronics from the University of Electronic Science and Technology of China (UESTC), Chengdu, China, in 2004 and 2009, respectively.

He is currently a full-time Professor with UESTC. His current research interests include high-temperature superconducting microwave circuits and systems, CAD, CAA, and production technology of high-temperature superconducting microwave circuits.

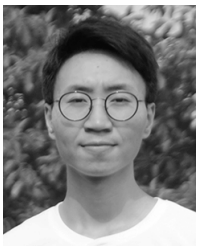

Zhihe Long was born in 1992. He received the B.E. degree in communications engineering from the Nanjing University of Science and Technology, Nanjing, China, in 2015. He is currently pursuing the master's degree in navigation, guidance, and control at the University of Electronic Science and Technology of China, Chengdu, China.

His current research interests include high-temperature superconducting microwave and millimeter-wave circuits and systems, and RFIC millimeter-wave phased arrays.

Liguo Zhou was born in 1987. He received the M.S. degree in electronic communication engineering from the University of Electronic Science and Technology of China, Chengdu, China, in 2016, where he is currently pursuing the Ph.D. degree in navigation, guidance, and control.

His current research interests include application technology of high-temperature superconductor and radio frequency and microwave technology.

Man Qiao was born in 1993. She received the B.S. degree from the Huaihua University of Electronic Science and Technology, Huaihua, China, in 2015. She is currently pursuing the master's degree in electronic communication engineering at the University of Electronic Science and Technology of China, Chengdu, china.

Her current research interests include radio frequency and microwave circuits and systems.

Fangyan Hou was born in 1990. He received the master's degree in communication engineering and electronic information engineering from the University of Electronic Science and Technology of China, Chengdu, China.

He is currently with Shanghai United Imaging Healthcare Co., Ltd., Shanghai, China. His current research interests include high-temperature superconducting microwave circuits and systems.

Mingen Tian was born in 1990. He received the master's degree in electronic communication engineering from the University of Electronic Science and Technology of China, Chengdu, China.

His current research interests include high-temperature superconducting microwave circuits and systems.